Clinical Result of Epicardial Pulmonary Vein Isolation (LAVIE) by Cryoablation as Concomitant Cardiac Operation and Clinical Application of New Ablation Device (KIRC-119 Infrared Coagulator) to Treat Atrial Fibrillation

Hiroshi Kubota[1], Kenichi Sudo[1], Shinichi Takamoto[2], Hidehito Endo[1],
Hiroshi Tsuchiya[1], Akihiro Yoshimoto, Yu Takahashi,
Yusuke Inaba[1] and Akira Furuse[3]
[1]Dpt of Cardiovascular Surgery, Kyorin University, Tokyo,
[2]Mitsui Memorial Hospital, Tokyo,
[3]JR Tokyo General Hospital, Tokyo,
Japan

1. Introduction

Maze surgery is widely used to treat atrial fibrillation but requires cardiopulmonary bypass and longer aortic cross-clamping time. Percutaneous transcatheter pulmonary vein isolation or catheter-based maze procedure are time consuming and relies on fluoroscopy and contrast media, and pulmonary vein obstruction and cardiac tamponade are still major problems. Although thoracoscopic minimally invasive epicardial pulmonary vein isolation using a radiofrequency device is also widely accepted, the device has the weakness to ablate the free wall of the atrium. To overcome these drawbacks, new ablation devices and techniques were developed using two kinds of energy source.

2. Epicardial cryoablation and epicardial infrared ablation

As energy sources, cryothermia and infrared were used. They were applied experimentally and clinically.

2.1 Epicardial cryoablation

First, to enable circumferential epicardial PV ablation, a hook-shaped cryoprobe was developed. Its efficacy was examined in canine model.

Second, a new operative procedure using a conventional cryo-system was also developed and applied clinically.

2.1.1 Epicardial pulmonary vein isolation with a hook-shaped cryoprobe to treat atrial fibrillation

After it was shown that a rapidly firing focus in a pulmonary vein (PV) can cause atrial fibrillation, percutaneous endocardial PV isolation (ablation) using radiofrequency became an established method of treatment. However, the technique is time consuming. It requires fluoroscopy and contrast media to identify the PV, and cardiac tamponade and PV stenosis (obstruction) are major complications. To overcome these drawbacks, we tried using cryoablation. Although the effectiveness of cryoablation has already been demonstrated in the modified maze procedure, its effectiveness by the epicardial approach in the beating heart was unknown. We developed a hook-shaped cryoprobe to circumferentially ablate PV orifices epicardially. The aim of this study was to confirm the efficacy of this method electrophysiologically in an experimental study in dogs.

We used a cryosurgical system PCG12R (CO_2, −60 degrees; Spembly Medical Ltd. Hampshire, UK) to create the cryolesions. A novel hook-shaped cryoprobe, 20-mm long and 3-mm wide, was developed to facilitate the PV ablation (Fig 1-A, B).

(A)   (B)

Fig. 1. The hook-shaped cryoprobe. (A) The hook is 20-mm long and 3-mm wide. (B) Thoracoscopic experiment using a canine model.

Material and methods

Five adult mongrel dogs weighing 14.2 ± 2.5 kg were anesthetized with ketamine hydrochloride (20 mg/kg, IM) and sodium pentobarbital (16 mg/kg, IV), and ventilated. The pericardium was opened through a median sternotomy, and the surrounding tissue was dissected to expose all PVs and their orifices into the left atrium. Since each dog had six or seven PVs, a total of 32 PVs were examined.

Before cryoablation, the pacing threshold of the left atrium was determined by stimulation with a bipolar electrode. Next, each PV was stimulated. The electrode was slid from the ostium to the distal site of the PV little by little, and the area of each PV that had the same pacing threshold as the left atrium was identified. Encircling cryoablation was then performed with the hook-shaped cryoprobe to circumferentially ablate the orifice of each PV epicardially. The circumferential cryolesions were created by passing the probe behind the orifice of the PV. The PV was compressed and flattened by pulling the probe upward when the cryoablation was done. The probe was applied to each orifice for 90 seconds (Fig 2, 3).

Chnges in PV potential

Before and during cryoablation, bipolar electrodes were placed on the PV, left atrium, left atrial appendage, and right atrium, and electrical potentials were recorded (n = 16). Two hours later, the electrical potentials were also recorded.

Changes in cardiac rhythm

Before and during ablation, bipolar electrodes were placed on the PV, left atrium, left atrial appendage, and right atrium, and the heart was paced through the electrode on the PV. The electrical potentials at each site were recorded (n = 16), and they were also recorded during PV pacing two hours later.
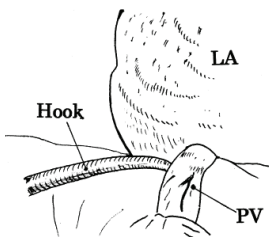
Fig. 2. Diagram of the area where cryoablation is performed with the assistance of the probe.
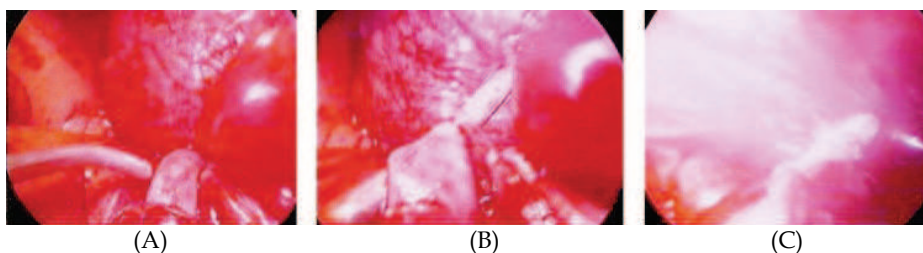(LA = left atrium; PV = pulmonary vein.)

(A)   (B)   (C)

Fig. 3. Procedure for creating a circumferential cryolesion (Thoracoscopic view).(A) The
probe is passed behind the PV and pulled upward. (B) The PV is compressed and flattened
by the probe. (C) Cryoablation is performed for 90 seconds.

Results
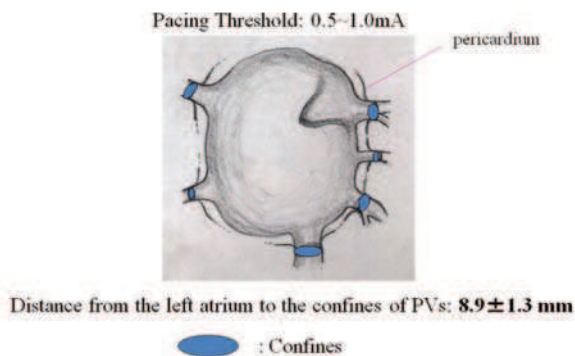The mean distance between the PV orifice and the pacing boundary was 8.9 ± 1.3 mm (Fig. 4).

Fig. 4. Electriphysiological characteristics of canine PVs
Canine PVs showed same electrophysiological characteristics as the atrium in some
extention.

All PVs had the same pacing threshold as the left atrium at some distance. Twenty-nine of
the pacing boundaries were present on the pericardial reflection or in the pleural cavity; the
pacing boundaries of only three PVs (left superior) were in the pericardial space. When a
pacing site was positioned beyond the boundary, the pacing threshold suddenly became
extremely high.

Immediately after commencing the cryoablation, the potential of the PV diminished (Fig. 5), and it had not recovered two hours later. Immediately after commencing the cryoablation, the cardiac rhythm converted from the pacing rhythm to the sinus rhythm (Fig. 6). The effectiveness of the ablation persisted two hours later.
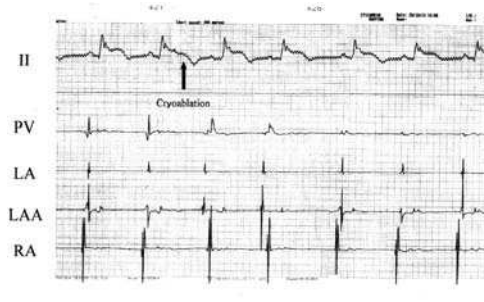

Fig. 5. Atrial and PV potentials during ablation (spontaneously beating heart).
Immediately after the start of cryoablation, the PV potential decreased rapidly and became almost flat. A couple of ectopic beats, which may have arisen from the cryosite, were observed. (LA = left atrium; LAA = left atrial appendage; PV = pulmonary vein; RA = right atrium.)

Fig. 6. Atrial and PV potentials during ablation (pacing from the PV).
Before ablation, pacing signals from the PV were conducted to both atria. Immediately after commencing the cryoablation, the cardiac rhythm converted from pacing rhythm to sinus rhythm. An ectopic potential (★), which may have arisen from the cryosite, is seen.

Comment

Radiofrequency endocardial PV ablation became widely adopted after reporting that rapidly firing foci could be identified in and around the PVs, and that ablation of such foci might lead to resolution of paroxysmal AF (Haissaguere et al., 1998; Pappone et al., 2000). However, the procedure depends on fluoroscopy and the use of contrast medium to identify the PVs. The electrophysiologic studies are time consuming, and cardiac tamponade and PV obstruction are still major problems. Our experiment was designed to overcome these problems.

We first investigated whether the PVs of mongrel dogs have the same electrophysiological characteristics as human PVs. Most dogs have 6 to 7 PVs, and a total of 32 PVs were studied. All PVs were found to have the same electrical characteristics as the left atrium at some distance, and almost all PVs had their electrical boundary on the pericardial reflection on the

PVs or after they passed into the thoracic cavity. Although no histopathologic examinations were performed in this study, these findings suggested that the myocardium extends into the PVs of dogs, the same as in humans. Based on these findings, we concluded that mongrel dogs could be used as a model to verify the efficacy of ablation.

The potential of the PVs diminished immediately after the start of ablation, and the PV pacing rhythm immediately converted to sinus rhythm. These phenomena demonstrate that the epicardial cryoablation had created a bidirectional conduction block. Although the irreversibility of the effectiveness of ablation was confirmed two hours later, a chronic study is needed to demonstrate the permanence of the effect of the cryolesion.

The effect of epicardial cryoablation does to not reach the endocardium of the beating heart, because the normothermic blood flow within it weakens the cryoeffect (Kubota, et al., 2002). However, we have shown that the cryoablation in the warm beating heart is effective only at sites that can be compressed by the cryoprobe, thereby eliminating blood flow with it. When the hook probe was pulled upward, the PV was flattened and the blood flow within it was completely eliminated. Flattening a PV can create a "local arrested heart," that may be why cryoablation is able to produce an encircling lesion in a "single" application and create a bidirectional electrical block at PV orifices. Although no histopathologic examinations were performed in our study, the electrophysiologicl findings suggest that the PV wall was ablated transmurally. These results of our preliminary experiment suggest that cryoablation is capable of overcoming some of the drawbacks of the percutaneous endocardial approach. Modification of the device will allow thoracoscopic epicardial ablation of the PVs (Kubota et al. 2004).

2.1.2 Epicardial pulmonary vein isolation by cryoablation as concomitant cardiac operation to treat nonvalvular atrial fibrillation: "LAVIE" procedure

How should patients with nonvalvular atrial fibrillation who require cardiac operation be managed? We developed an epicardial technique to isolate the left atrial posterior wall and pulmonary veins. The first clinical case is presented and postoperative clinical course of 16 patients' series are described.

Case presentation

On March 29, 2001, an 82-year-old woman was transferred to our hospital with a diagnosis of acute aortic dissection, DeBakey II, Stanford A. Preoperative echocardiography revealed normal cardiac function, and aortic regurgitation was trivial. There was no mitral regurgitation and no enlargement of the left atrium. A preoperative electrocardiogram showed AF, and the amplitude of the f-wave in V_1 was 0.1 mV. The patient's AF had initially been diagnosed about 3 years previously. An operation was performed on the day after admission.

The pericardium was opened through a median sternotomy. A mild bloody pericardial effusion was aspirated, and tapes were passed around the SVCand the IVC. A cardiopulmonary bypass was established by cannulations through the left femoral artery and both vena cavae, and the left ventricle was vented through the right superior PV. During cooling, the tissue behind the SVC and IVC was carefully dissected to expose the left atrium. When the tympanic temperature reached 20°C, both vena cavae were snared, and epicardial cryoablation was started with N_2O at −60 °C (Cardiac Cryosurgical System CCS-200; Cooper Surgical, Shelton, CT). A pencil-type probe (20 mm × 9 mm) and a T-shaped probe (20 mm × 5 mm) were used. The right side of the left atrium was cryoablated first. The roof of the left atrium behind the SVC was then ablated by pulling the snared tape anteriorly, and the left atrium behind the IVC was ablated pulling the snared tape anteriorly (Fig 7A). At a tympanic temperature of 18°C, the ascending aorta was incised under circulatory arrest and retrograde cerebral perfusion. Antegrade blood cardioplegia was

infused. A 26-mm woven Dacron graft (Hemashield®, Boston Scientific Medi–Tech, Wayne, NJ) was anastomosed. The graft was clamped, and the antegrade perfusion was started through a side branch of the graft. The retro-aortic portion of the left atrial roof was easily cryoablated because the proximal ascending aorta was left transected. Reinforcement of the proximal aorta and an anastomosis were carried out. The cryoablation of the remaining part of the left atrium was continued while warming. A tape was passed around the pulmonary artery, and as the tape was pulled anteriorly, the cryoprobe was passed into the transverse sinus, thereby enabling ablation of the left side of the roof of the left atrium. Great care was taken not to ablate the left coronary artery system to prevent reactive hypertrophy of the intima, which might cause serious ischemia of the myocardium. The ablation was extended to the left side of the left atrium, the inferior wall of the left atrium parallel to the coronary sinus, and was finally connected to the retro-IVC lesion that had been made before circulatory arrest (Fig 7B, C). The left atrial appendage was ligated, and the orifices of the left superior and inferior pulmonary vein were cryoablated (Fig 7D). All applications of the probe were epicardial, and the cryolesions were always created so that they overlapped by 2～3 mm to produce a continuous lesion. The duration of each application was 1.5 minutes.
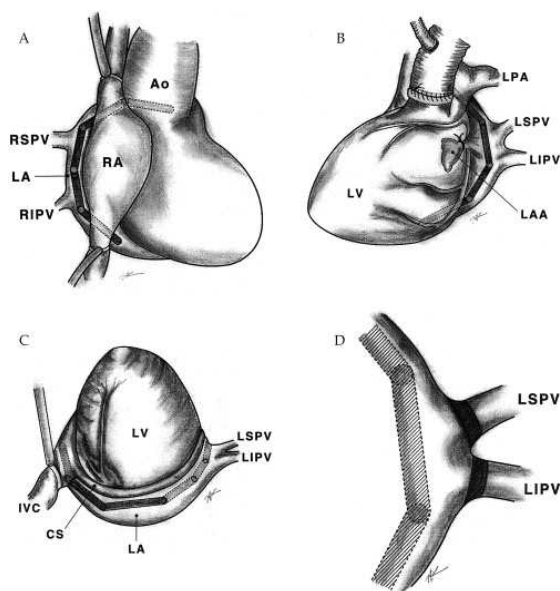

Fig. 7. Epicardial encircling cryoablation of the left atrium.

The cryolesions were made with 2~3 mm overlaps to obtain a continuous linear lesion. The duration of each application was 1.5 min. Two kinds of cryoprobe were used. (A) Tapes were passed around the SVC and the IVC. The right side of the left atrium was cryoablated. The left atrium behind the IVC and the roof of the left atrium behind the SVC were ablated while the snared tape was pulled anteriorly. (B) Before the proximal anastomosis, the retro-aortic portion of the left atrium was ablated. The cryoablation of the remaining part of the left atrium was continued while warming. Great care should be taken not to ablate the left coronary artery. The ablation was extended to the left side of the left atrium. (C) The inferior wall of the left atrium parallel to the coronary sinus was ablated and it was connected to the retro IVC lesion that was made before circulatory arrest. (D) The left atrial appendage was

ligated. The orifices of the left superior and inferior pulmonary vein were cryoablated respectively. (LPA; left pulmonary artery, CS; coronary sinus)

The heart beat recovered spontaneously and was in sinus rhythm from the start. Weaning from the cardiopulmonary bypass was easy. Total cardiopulmonary bypass time was 199 minutes. Aortic cross-clamping time was 99 minutes. Circulatory arrest time was 40 minutes. Operation time was 5 hours.

The patient was extubated the next day and returned to a general ward on postoperative day 2. The postoperative electrophysiological examination revealed that overdrive pacing inside of the encircling lesion with a bipolar pacing wire left behind the left atrium did not affect the cardiac rhythm, even when the output was set at maximum (Fig. 8). Atrial electrical potential within the encircling lesion was recorded with the same pacing wire, and no atrial potential was found within the encircling lesion. A Holter electrocardiogram recorded 4 months after the operation showed a regular sinus rhythm without any supraventricular tachycardia. The patient is alive and well, an electrocardiogram ten years after the operation showed that the regular sinus rhythm had been maintained without drugs.
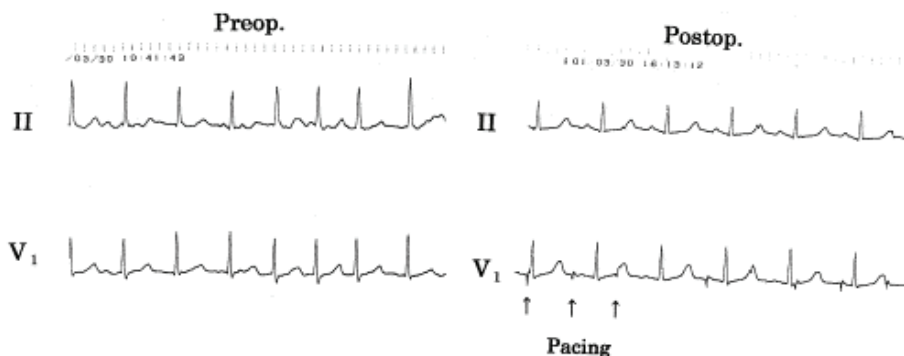

Fig. 8. Postoperative electrophysiological study.
When the posterior wall inside the encircling lesion was paced, pacing failed to affect the cardiac rhythm.

Comment

The maze procedure is usually performed to treat AF secondary to atrial overload mainly caused by valvular disease and is not commonly used to treat paroxysmal or lone AF because full sternotomy, cardiopulmonary bypass, and dual atriotomy are too invasive. On the other hand, we are often faced with elderly patients who are surgical candidates and have AF plus nonmitral disease (eg, coronary artery disease, aortic stenosis, aortic dissection, and aortic aneurysm). Until now we have tended not to perform the maze procedure concomitant with operation for the primary disease in such patients because it prolongs aortic cross-clamp time and requires additional atriotomy. To overcome these problems, we developed the technique previously described and called it the "LAVIE" (left atrium and vein isolation: epicardial) procedure. Although a preoperative electrophysiological study was not performed, in view of the patient's advanced age and echocardiographic findings her AF was thought to be lone AF, very probably of the pulmonary vein origin. The postoperative electrophysiological study showed that the encircling pulmonary vein lesion had produced a bi-directional block. The posterior wall of the left atrium, including the pulmonary veins, had been electrically isolated. We added the cryoablation of the orifice of the left pulmonary veins to isolate the ectopic focus with greater certainty. In nonopen cardiac operation, such as coronary bypass procedures, the

entire length of the left atrial roof can be ablated by pulling up a tape passed around the ascending aorta and the pulmonary trunk through the transverse sinus.

The left atrium and vein isolation technique does not require atriotomy and does not prolong the aortic cross-clamp time. Since two cryoprobes can be used simultaneously, total ablation time can be shortened. Both vena cavae were snared to reduce blood flow in the left atrium. Reducing the blood flow, which weakens the cryo effect, is quite important to producing transmural cryolesions. The left ventricular venting is also effective to reduce the blood in the left atrium. This technique should be applied only during cardiac operations with total cardiopulmonary bypass (Kubota et al., 2003).

2.1.3 Clinical result of epicardial pulmonary vein isolation (LAVIE) by cryoablation as concomitant cardiac operation to treat atrial fibrillation

From April 2002 to April 2010, 16 patients underwent LAVIE technique concomitant with non-valvular cardiac operation. The primary diseases were: coronary artery disease, acute aortic dissection, and aortic stenosis. The conversion ratio to sustained sinus rhythm was verified and compared with the result of modified Kosakai maze procedure performed in the same period.

Results: The postoperative EPS revealed that overdrive pacing from inside of the box lesion did not affect the cardiac rhythm, and no atrial potential was found within the lesion (Fig. 9). Sustained sinus rhythm, including atrial-based paced rhythm was present in 75.0 % in LAVIE performed patients.
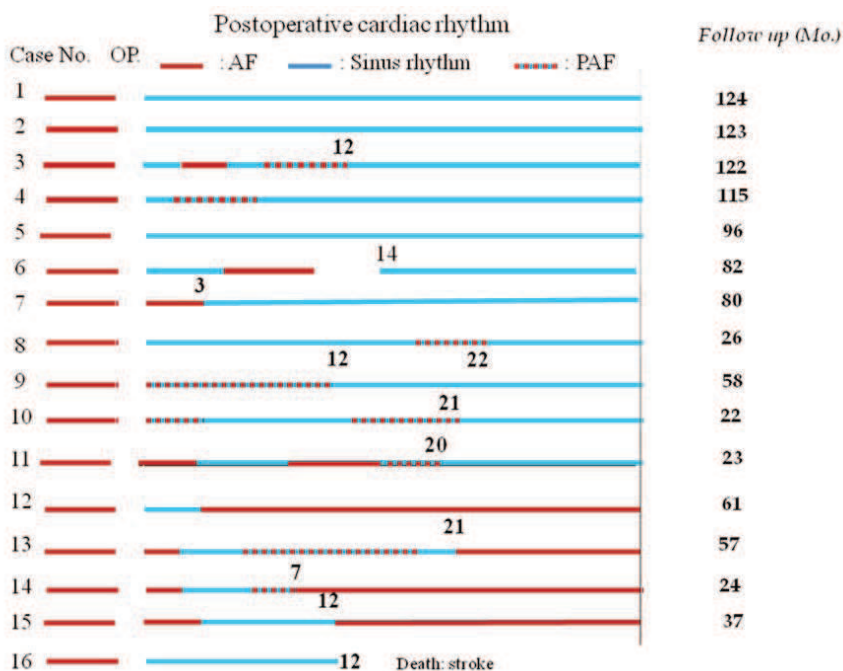

Fig. 9. Postoperative cardiac rhythm after "LAVIE" procedure
Sinus rhythm was restored in 75%. Note that in eight patients, after the "irritable" period, stable sinus rhythm restored.

2.2 Epicardial infrared ablation

Infrared is one of the effective energy sources to ablate the myocardium. To realize transmural atrial ablation, KIRC-119 was developed. Its efficacy was examined in canine model and applied clinically.

2.2.1 Fundamental experiment of atrial ablation using a prototype infrared coagulator

The ideal method for atrial ablation has not yet been reported. In the infrared coagulator, the distal exit plane of the light-conducting rod is connected to a tip. We made three kinds of artificial sapphire tips for this device to obtain linear photocoagulation. When each tip is touched to the epicardium, light energy is absorbed by the myocardium, which becomes photocoagulated. In this study, the characteristics of the three kinds of tip were first compared in a canine heart. The depth and width of the myocardial lesions were measured, and their histopathologic features were observed. Changes in the atrial conducting pathway immediately after and 3 months after ablation then were recorded by epicardial mapping.

Material and methods

The IRK-151 infrared coagulator (Infrarot-Kontaktkoagulator; Messerschmidt-Bolkow-Blohn, Frankfurt, Germany) was originally developed to secure hemostasis in bleeding parenchyma as an alternative to high-frequency electrocoagulation or laser coagulation (Fig 10A). The single-application time is limited to within 3 seconds by a timer. In this device, light from a tungsten-halogen lamp is focused by a reflector into a light-conducting quartz rod with a diameter of 10 mm. It emerges as 35 W/cm2 of near-infrared light energy (wavelength, 400 to 1600 nm; peak wavelength, 850 nm). The distal exit plane of the light-conducting rod is connected to the tip. We made three kinds of original tips using artificial sapphire (tapered, coated, and angled) by polishing the surface of a cylindrical sapphire slantwise (Fig 10B). All the tips have a rectangular (1.5 × 10.0 mm) edge to allow linear atrial myocardial ablation.

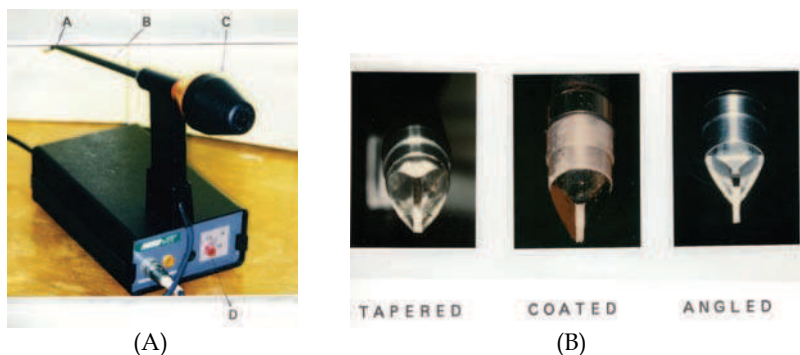(A)   (B)

Fig. 10. (A) The IRK-151 infrared coagulator (a = tip; b = light-conducting quartz rod; c = reflector; d = timer). (B) Three kinds of artificial sapphire tips: (left) tapered, (middle) coated, and (right) angled. The coated tip has the same shape as the tapered tip, but the slanting surfaces are coated with nickel and tin dichloride. The angled tip has a 4-mm straight nose to prevent unnecessary ablation caused by direct contact of the slanting surface. When these sapphire tips are pressed into tissue, light energy is absorbed by the myocardium, which is then photocoagulated.

The coated tip has the same shape as the tapered tip, and the slanting surfaces are coated with nickel and tin dichloride to prevent leakage of unnecessary energy in a lateral

direction. The angled tip has a 4-mm straight nose to prevent unnecessary ablation resulting from direct contact with the slanting surface.

Methods

Developing a suitable tip for obtaining linear atrial ablation

Nine adult mongrel dogs weighing 13.5 ± 1.7 kg were anesthetized using ketemine hydrochloride (20 mg/kg) intramuscularly and sodium pentobarbital (16 mg/kg) intravenously and were ventilated. Through a right thoracotomy, the beating right ventricular myocardium was ablated using the IRK-151 from the epicardium. The tip was compressed 2 to 3 mm into the epicardium unless this induced paroxysmal ventricular contraction. Four lesions were created using different durations of application (3, 9, 15 and 21 seconds). The three different sapphire tips were applied to 3 dogs each. Therefore, a total of 36 lesions were created. After ablation, the hearts were rapidly excised and the myocardium was fixed in 10% formalin. After adequate fixation, thin sections were cut and stained (hematoxylin-eosin and azan). The width, depth, and shape of ablation, and the resulting histopathologic changes were observed by light microscopy. To obtain linear coagulation, the ideal tip should create deep and narrow coagulation. Therefore we devised the linear index, to describe this: Linear index=depth of coagulation/width of coagulation. The linear indices using the three kinds of tips at 21 seconds of application were calculated and compared for each tip. Ventricular myocardium was used instead of atrial myocardium to assess the depth of coagulation because the atrial myocardium is too thin for this evaluation.

To evaluate the influence of tip pressure on the epicardium, the depth of the lesion when the tapered tip was compressed 2 to 3 mm into the epicardium and that when the same tip merely touched the epicardium were compared for various durations of application (3, 9, 15 and 21 seconds) using 3 adult dogs.

Atrial ablation with an infrared coagulator

In 3 dogs a linear lesion on the beating right atrial free wall was created from the annulus of the tricuspid valve to the intraatrial sulcus by using the tapered tip. This lesion was created by several overlapping applications (15 seconds for each application) from both the epicardial and endocardial sides (Fig.11). First, the endocardial ablation was performed by insertion of the light-conducting rod into the right atrium through a purse-string suture on the right atrial appendage. After that, epicardial ablation was performed on the same line as endocardial ablation. To ensure complete coverage, 2.0 mm of overlapped lesions were made. Before and after ablation, epicardial plaque–electrode mapping (24-channel bipolar electrodes, 33 × 45 mm) was performed to determine the conduction pathway in the right atrial free wall. The recording conditions were spontaneous beating and overdrive pacing from the low right atrium (R = 140/min). In two other dogs, the same line as that to be ablated was clamped with a Satynsky clamp. The atrial wall was then cut and sutured. After unclamping, epicardial mapping was performed in the same way. The result of postablation epicardial mapping was contrasted with the mapping of the cut and sutured atrial wall. The collected data were recorded and analyzed by the HPM-7100 mapping system (Fukuda Denshi, Tokyo, Japan). After the experiment, the chest wall was closed. Three months later, right atrial epicardial plaque–electrode mapping was performed again through another thoracotomy. After the completion of mapping, the right atrial free wall was excised, fixed, and stained in the same way as the ventricle, and the histopathologic changes were observed by light microscopy.
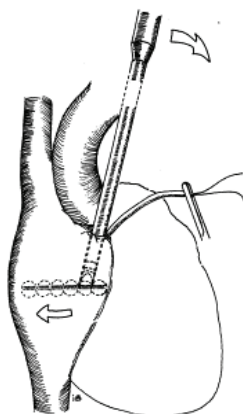
Fig. 11. A linear lesion was created by several overlapping applications from both the epicardial and endocardial sides.

Results

Developing a suitable tip for obtaining linear atrial ablation

Depth of lesion

The depth of the lesion was correlated with increased coagulation time (Fig. 12). The maximum depth was 10.3 ± 0.8 mm at 21 seconds using the tapered tip, which was significantly deeper than with the other kinds of tips. The depth of the lesion using the angled tip was 5.2 ± 0.3 mm, and that with the coated tip was 7.7 ± 0.3 mm at 21 seconds.
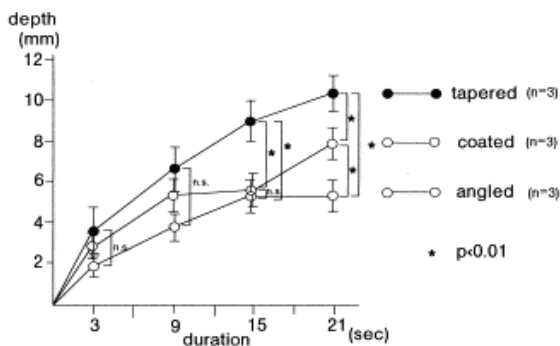
Fig. 12. Average depth of the lesion.
The maximum average depth of the lesion was 10.3 ± 0.8 mm at 21 seconds with use of the tapered tip. (n.s. = not significant.)

Width of lesion

The narrowest lesion width, 13.7 ± 1.5 mm at 21 seconds of ablation (Table 1), was created by the tapered tip. The linear index obtained using the tapered tip (0.76 ± 0.13 mm) was higher than that for the other tips (angled tip, 0.25 ± 0.02 mm; coated tip, 0.43 ± 0.03 mm).

Tip	Depth (mm)	Width (mm)	Linear Index[b]	n
Angled	5.2 ± 0.3	21.0 ± 1.0	0.25 ± 0.02	3
Coated	7.7 ± 0.3	18.0 ± 1.0	0.43 ± 0.03	3
Tapered	10.3 ± 0.8	13.7 ± 1.5	0.76 ± 0.13	3

[a] All comparisons between tips were statistically significant ($p < 0.05$).
[b] Linear index = myocardial depth of lesion/epicardial width of lesion.

Table 1. Lesion Measurements and Linear Indexa

Shape of lesion
Longitudinal sections showed that the longitudinal length of the lesions created by the three kinds of tips was preserved from the surface to the bottom. The cross-section of the lesion created by the tapered tip showed an elliptical shape. The coated tip created a cone-shaped lesion and the angled tip created a convex lesion at the center (Fig. 13).
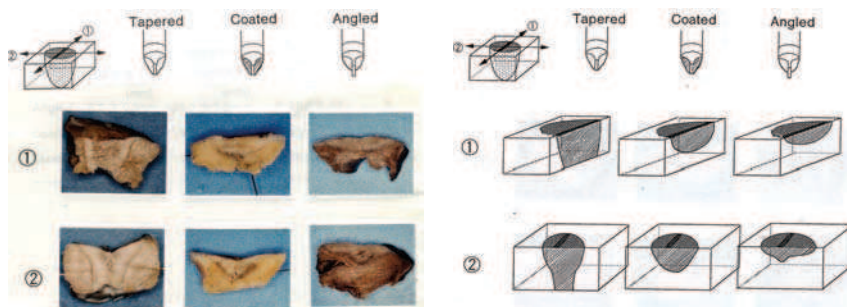
Fig. 13. Three kind of tips and shape of the lesion of the canine right ventricle
The cross-section of the lesion created by the tapered tip showed a transmural lesion.

Influence of tip pressure on the epicardium
When the probe merely touched the epicardium, the maximum depth of the lesion was 5.7 ± 0.3 mm at 21 seconds. By compressing the tip into the epicardium, it was possible to obtain a maximum of 1.8 times this depth at 21 seconds of ablation (Fig. 14).
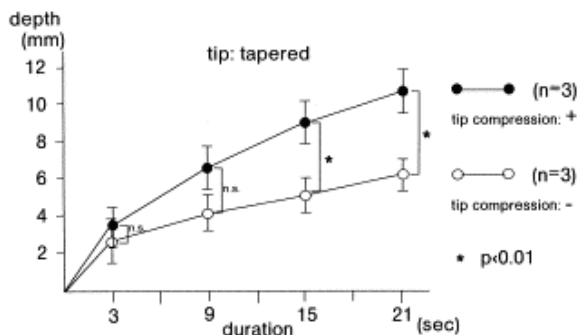

Fig. 14. Influence of tip pressure on the epicardium.
When the tip was pressed into the epicardium, the deeper lesion was created.

Histopathologic findings

The epicardium was preserved, and the ablated myocardium had well-demarcated photocoagulation necrosis without carbonization or vaporization. The nuclei of the myocardial fibers were concentrated. The myocardial fibers were atrophic and degenerated. The fundamental histopathologic structure was the same irrespective of whether ablation time was short or long (Fig. 15). All of the vessels were patent.
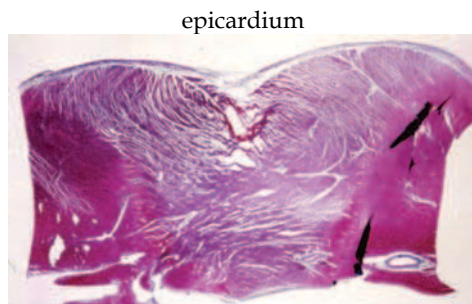
epicardium

Fig. 15. Histopathologic findings of ventricular myocardium.
The ablated myocardium had well-demarcated photocoagulation. The vessels were patent.
The lesion reached the endocardium with use of the tapered tip at 21 seconds.

Epicardial mapping

Before linear ablation on the right atrial wall, electrical potential was conducted regularly from the sinus node. After ablation, it was conducted from the node to the annulus of the tricuspid valve through the lateral side (intraatrial sulcus side) of the ablation area. Under overdrive pacing from the low right atrium, it was conducted from the low right atrium to the right atrial appendage through the lateral side of the ablation area (Fig. 16). Mapping after cutting and suturing the atrial wall showed the same pattern of conduction. Mapping 3 months after ablation also showed the same pattern of conduction.

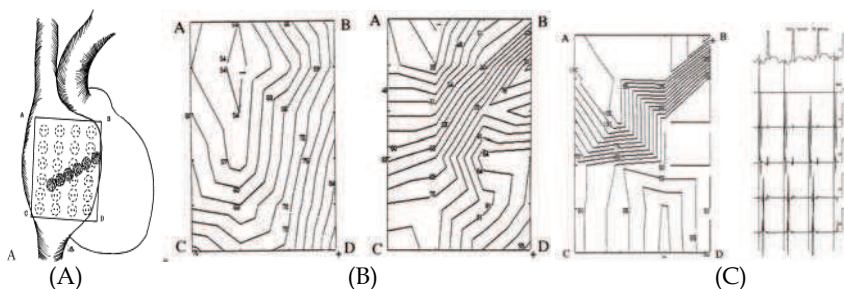

(A)   (B)   (C)

Fig. 16. Right atrial epicardial mapping
(A). Location of the electrodes. (B) The preablation map (left) and the postablation map (right) (sinus rhythm). The electrical conduction of the right atrium was blocked by the linear zone of photocoagulation. (C) Right atrial epicardial mapping (overdrive pacing from the low right atrium) (left) and electrocardiogram (right). Electrical potential conducted from the low right atrium to the right atrial appendage. The electrical conduction was blocked by the same area as in B. Electrodes 17 and 18 were on the lower side, and 19 and 20 were on the higher side near the lesions.

Histopathologic findings

The atrial epicardium was preserved. The ablated myocardium had well-demarcated transmural photocoagulation necrosis without carbonization or vaporization, as in the ventricular myocardium. The deposition of hemosiderin, invasion of macrophages, increased capillary vessels, and increased juvenile elastic fibers were observed in chronic phase. The myocardium did not revive. The endocardium was thickened, and elastic fibers also appeared (Fig. 17).
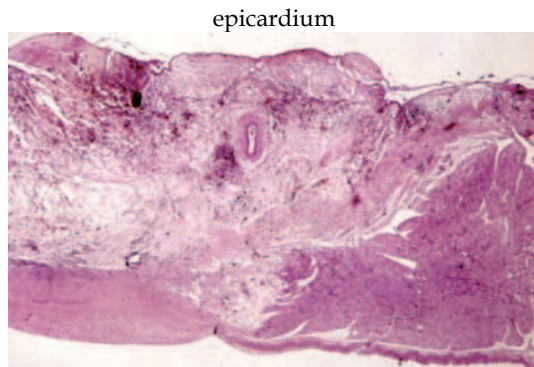
epicardium

Fig. 17. Right atrial free wall 3 month after ablation
The endocardium was thickened. Density of juvenile elastic fibers was higher. The vessels were patent.

Comment

Since the maze procedure for treating atrial fibrillation was published (Cox et al., 1991), surgical treatment for atrial fibrillation has attracted considerable attention and become widespread.

An IRK-151 infrared coagulator was developed in Germany (Nath et al., 1976). In relation to arrhythmia, The electrocardiographic changes after photocoagulation using the IRK-151 were examined on sinus node, right bundle branch, and His bundle in canine heart (Nakajima, et al., 1982). Because the atrial wall is thinner than the ventricular wall, atrial coagulation should not cause carbonization or vaporization, to prevent perforation. In our experiment, infrared photocoagulation caused well-demarcated and homogeneous necrosis within the lesions, without carbonization or vaporization, and the epicardium remained intact. Comparison of precoagulation and postcoagulation atrial epicardial electrode mapping confirmed that transmural degeneration of the atrial wall caused electrical block concurrently.

Linear ablation is more efficient than continuous overlapped ablation with a round tip. Usually, the volume of the lesion is calculated according to a formula using the epicardial radius (a) and myocardial depth (b): Volume (oblate)=$(1/2)(4/3) \pi a^2 b$, and Volume (prolate)=$(1/2)(4/3) \pi ab^2$, where for oblate, a > b and for prolate, a < b (Holman et al., 1983, Markovitz et al., 1988). This formula is not suitable for evaluating the efficacy of linear ablation as it is neither oblate nor prolate. A compact index (linear index=myocardial depth of lesion [mm]/epicardial width of lesion [mm]) was therefore devised. As the index increases, the ablation approaches linearity. Unexpectedly the tapered tip showed the highest index (0.76), and the coated tip the lowest index (0.43). This result may have

occurred because the nickel and tin dichloride coating the surface could not reflect the infrared rays perfectly, leading to heating of the tip surface. The degree of tip pressure on the myocardium is also important for determining the depth of the lesion. Our experiment showed that compressing the myocardium created a deeper lesion than merely touching it. The argon laser and neodymium:yttrium-aluminum garnet laser are used clinically for treatment of arrhythmia (Hendry et al., 1993, Svenson et al., 1987). These instruments are expensive and large, and it is difficult to obtain linear ablation. Furthermore, lasers may cause perforation of the thin atrial wall. The IRK-151 infrared coagulator produces well-demarcated lesions that are easily detected with the naked eye and whose depth is controllable by adjusting the duration of application. The depth was found to be adequate for atrial ablation aimed at blocking the conduction pathway. An average depth of 5 mm is created when a cryoprobe is applied to perfused dog epicardium for 90 to 120 seconds (Mikat E. et al., 1977). When the infrared coagulator was used, it took only 6 seconds to obtain the same depth of the lesion. The infrared-maze procedure can be done in a short time compared with the cryo-maze. Although the maximum length of the cryolesion at one application is 15mm, the infrared coagulator is capable to elongate the lesion length at one application by modifying the shape of the sapphire tip, light-conducting rod, and a reflector (Kubota et al., 1998).

2.2.2 Conventional maze procedure using an IRK- 151 infrared coagulator in canine model

The IRK- 151 infrared coagulator was employed to electrophysiologicany confirm the efficacy of this device under arrested heart in canine model.

Methods. The MAZE-Ill procedure was performed in four mongrel dogs. Instead of a pulmonary vein-encircling incision, IRK-151 was applied endocardially to create a continuououusly overlapping circular lesion under the arrested heart using a cardiopulmonary bypass. After aortic declamping, the potentials of both atria were recorded using 18 bipolar electrodes implanted in the atrial wall (Fig. 18). The recording conditions were: 1) sinus rhytlm, 2) overdrive pacing from outside the encircling coagulation, and 3) overdrive pacing from inside the encircling coagulation. After the experiment, the bronchus and esophagus behind the coagulation point were excised, fixed and stained (HE, Azan).
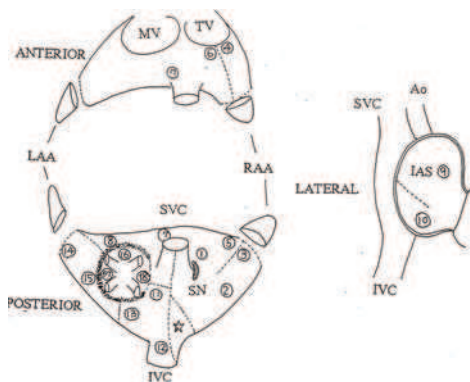

Fig. 18. Sites of electrodes
Inserted sites of eighteen bipolar electrodes are shown.

Results.

The mean aortic cross-clamping time was 26±10 min. The total infrared coagulation time was 4.1±0.6 min.

1) There was no detectable potential with the pulmonary vein-encircling coagulation. 2) There was no conduction of paced atrial potential inside the encircling coagulation. 3) Only the area within the encircling coagulation was activated by the stimulus. Other parts of the atrium showed sinus rhythm simultaneously (Fig. 19 A, B, C).
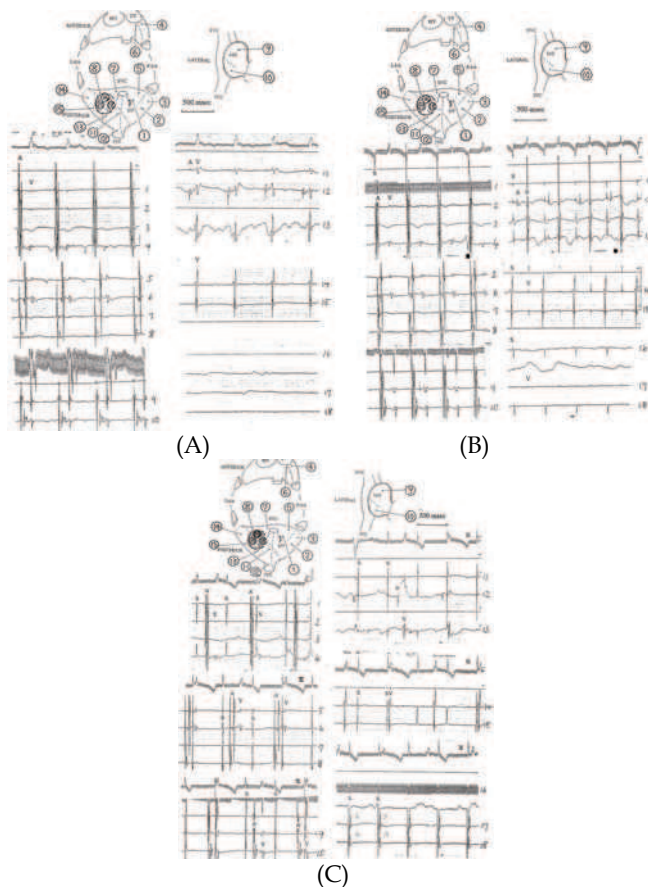

(A)   (B)

(C)

Fig. 19. Atrial potentials recorded by multi-electrodes after endocardial PV-encircling ablation (A) With the heart beating spontaneously, electrode no. 1 was the earliest activating point. The synchronous atrial potentials were detected in electrodes nos. 2-12. With electrodes nos. 13-18, no atrial potentials were detected. (B) With stimulation by electrode no. 1 (S-S interval: 500 msec), synchronous atrial potentials were detectedby electrodes nos. 1-13. No atrial potentials were detected by electrodes nos. 16-18. (C) With stimulation by electrode no. 16 (S-S interval: 500 msec), synchronous atrial potentials were detected by electrodes nos. 17 and 18. Electrodes nos 1-12 showed sinus rhythm. The bronchus and the esophagus near behind the coagulated left atrium showed no histopathological change.

Comment

Based on above results, it can be said that the pulmonary vein encircling area could be electrically isolated by endocardial coagulation under the cardioplegic arrested heart without collateral tissue damage (Kubota et al., 2000).

2.2.3 Epicardial maze procedure on the beating heart with an infrared coagulator KIRC-119

To make the treatment of AF less invasive, we applied this device to epicardial maze procedure on the beating heart in canine model, and in this study we attempted to electrophysiologically and pathologically confirm the efficacy of the method.

Material and Methods

Because the original IRK-151 contains a 3-second timer and the plastic body of the IRK-151 is not strong enough to tolerate the long coagulation time, we modified the coagulator to make it strong enough for atrial ablation by substituting a 40-second timer and changing the body from plastic to metal (Fig. 20).

Fig. 20. KIRC-119: the plastic body has been replaced by a metal body to enable it to tolerate the long duration of the coagulation

Five mongrel dogs weighing 14.5 ± 2.3 kg were anesthesized with ketamine hydrochloride (20 mg/kg, intramuscularly) and sodium pentobarbital (16 mg/kg, intravenously), and were ventilated. After median sternotomy, both pleural cavities are openand the vagal nerves are exposed. The pericardium was then opened, and a bipolar electrode was attached to the right atrium. Sustained AF was induced preoperatively by bilateral vagal nerve stimulation (pulse width 0.2 ms, 3 V, 10 Hz) followed by 2 hours of burst stimulation of the atrium. A tape was passed around the SVC, another around the IVC, and a third around the ascending aorta and the main pulmonary artery through the transverse sinus. The tissue behind the SVC and IVC was carefully dissected to expose the left atrium; and after ligating and dividing the azygos vein, the infrared coagulation was performed. Instead of all the incisions of the maze III procedure, except the intraatrial septal incision, the infrared coagulator was applied epicardially to create continuous overlapping linear lesions. The duration of application for each ablation was 9 seconds, and a 10-mm lesion was created. After completion of all of the lesions, 11 bipolar electrodes were attached to the wall of each

atrium (Fig 21 A). An electrocardiogram (ECG) and atrial potentials were recorded with an HPM 4500 polygraph (Fukuda Denshi, Tokyo, Japan).
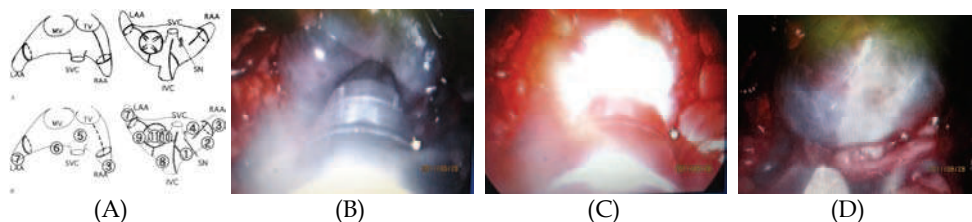

| (A) | (B) | (C) | (D) |

Fig. 21. Lesion pattern and thoraciscopic view of infrared ablation
(A) Coagulation was performed along the incision line of the Maze III procedure, except intraatrial septal incision. After the procedure, 11 bipolar electrodes were placed in the atrial wall, and the potentials were recorded. (B-D) After the infrared ablation, atral free wall was discolored.

The recording conditions were as follows: (1) spontaneous beating; (2) overdrive pacing from the right atrial appendage (RAA); (3) overdrive pacing from the left atrial appendage (LAA); and (4) overdrive pacing from inside the PV encircling lesion.
After recording the atrial potentials, burst stimulation was applied in an attempt to induce AF. If it failed the first time, we tried two more times. After the experiment, the coagulated left atrial wall was excised, fixed, and stained (hematoxylin-eosin, AZAN), and histologic sections were examined microscopically.
Results
No potentials were detectable within the RAA, LAA, or PV encircling lesion during spontaneous beating, but other areas of the atrium exhibited sinus rhythm (Fig. 22 A). During overdrive pacing from the RAA, the atrial potential subsequent to the pacing was detected only in the RAA. Other areas exhibited sinus rhythm (Fig. 22 B). During overdrive pacing from the LAA, only the area within the LAA lesion was activated by the stimulus. Other areas exhibited sinus rhythm (Fig 22 C). During overdrive pacing from inside the PV encircling lesion, only the area within the PV encircling lesion was activated by the stimulus. Other areas exhibited sinus rhythm (Fig 22 D)
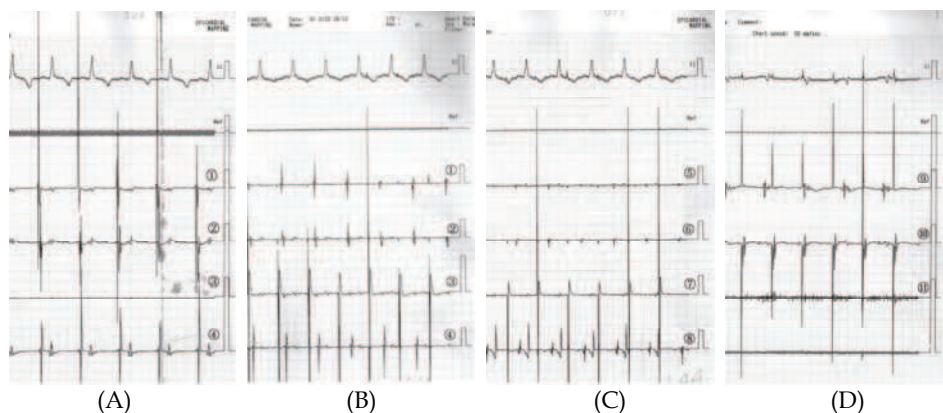

| (A) | (B) | (C) | (D) |

Fig. 22. Atrial potential recorded by multi-electrodes.

(A) Atrial potential during spontaneous beating. No potential was detected within the right atrial appendage ([RAA] electrode no. 3). Other areas of the atrium exhibited sinus rhythm. No potentials were detected with the electrodes within the left atrial appendage (LAA) or pulmonary vein (PV) encircling lesion (electrodes nos. 7, 10, and 11) either. (B) During overdrive pacing from the RAA (electrode no. 3), only the area within the RAA lesion was activated by the stimulus. Other areas exhibited sinus rhythm.

(C) During overdrive pacing from the LAA (electrode no. 7), only the area within the LAA lesion was activated by the stimulus. Other areas exhibited sinus rhythm. (D) During overdrive pacing from inside the PV encircling lesion, only the area within the PV encircling lesion (electrode no. 10) was activated by the stimulus. Other areas exhibited sinus rhythm. Electrode no. 11 was used to stimulate the atrium.

None of the three areas inside the encircling lesion exhibited any potentials during sinus rhythm, and only these lesions were activated by the overdrive stimulus from inside the lesions. Other areas always exhibited sinus rhythm with or without the pacing from inside the encircling lesions. Although we tried to induce AF three times in each dog after completing the ablation, burst stimulation failed to induce AF in any of the dogs. Histologic examination showed preservation of both the endocardium and epicardium of the coagulated lesion. Well-demarcated transmurally degenerated myocardium was demonstrated (Fig.23).
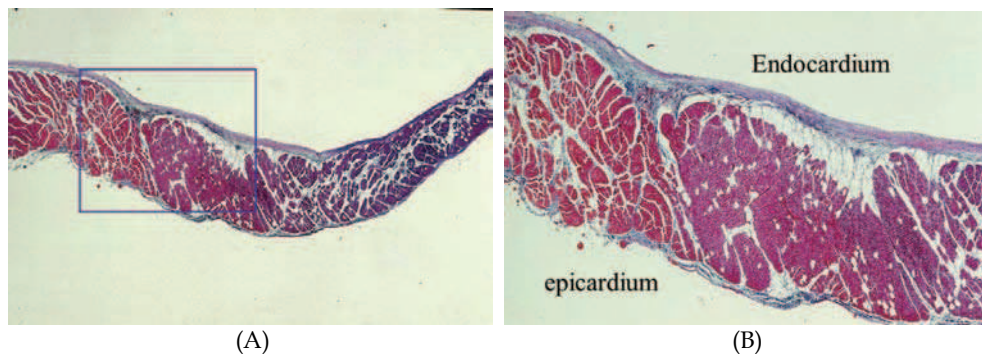

| (A) | (B) |

Fig. 23. Histologic changes in the left atrium.
(A) Well-demarcated transmurally degenerated myocardium was demonstrated. Both the endocardium and the epicardium were intact. (B) High-power field.

Burst stimulation did not induce AF in any of the dogs. No ST-T changes or arrhythmias occurred during ablation.

Comment

Is the warm beating heart more suitable for infrared coagulation than the cardioplegic arrested heart? The depth, width, and volume of the myocardium coagulated with a Nd-YAG laser were compared in the warm red beating heart and in the cold white nonbeating heart infused with 0°C saline (cardioplegic model) through the coronary artery (Ohtake et al., 1992). The depth, width, and volume of red myocardium coagulated were significantly greater than in the white myocardium, and the volume of white myocardium coagulated was about 60% of the volume of the red myocardium that was coagulated. They concluded that Nd-YAG laser energy was absorbed by the blood (red color indicates hemoglobin) and

that a higher temperature was transmitted to the myocardium. Accordingly, because infrared rays are capable of producing photocoagulation that is equivalent to laser coagulation, the beating heart is preferable for obtaining efficient myocardial coagulation with infrared rays.

To develop a new ablation device, it is important to preserve the endocardium to prevent thromboembolism. Histologic examination revealed photonecrosis in the ablated myocardium without carbonization or vaporization, and the epicardium and the endocardium were intact. The photoenergy passes through them because both of them are translucent and when the energy reaches the myocardium, a higher temperature is transmitted. There are three encircling lesions in our procedure, one each in the RAA, LAA, and PV encircling lesion. All three lesions in our experiment were confirmed to be isolated electrophysiologically in all dogs, suggesting that the coagulator is capable of being used to make continuous transmural lesions in both atria. The intraatrial septum was not ablated in our procedure because cardiopulmonary bypass is necessary to expose the intraatrial septum. Although the contribution of the intraatrial incision to the effectiveness of the maze procedure is not well known, omitting the intraatrial ablation in our experiment did not interfere with prevention of AF induction. Vagus nerve and atrial burst stimulation were used to create a model of AF. Since the earliest mRNA induction that modifies the atrial potassium channel and shortens the atrial refractory period begins only 30 minutes after continuous burst stimulation (Yamashita et al., 2000), we tried creating a model of AF induced by vagus nerve stimulation followed by 2 hours of burst stimulation before ablation. A model of stable sustained AF was achieved in all dogs by this procedure, and it improved the reliability of our experiment in demonstrating the efficacy of the treatment of AF (Kubota et al., 2004).

2.2.4 Epicardial electrical isolation of the right atrial appendage on the beating heart with an infrared coagulator KIRC-119

We present a 1st case in which the infrared coagulator was used clinically on the patient's beating heart.

Case presentation

On August 25, 2005, a 63-year-old man was referred to our hospital because of a complaint of chest oppression. He was diagnosed with unstable angina pectoris. Emergency coronary angiography revealed 75% stenosis of the left main trunk, 60% stenosis of the proximal left anterior descending artery, and 60% stenosis of the middle portion of the left circumflex artery. The left ventricular ejection fraction was 0.40. Echocardiography showed anteroseptal hypokinesis of the left ventricle but no valvular dysfunction. The diameter of the left atrium was 34 mm. The electrocardiogram (ECG) showed ST depression in leads II, III, aVF, and V_2 through V_6. No Q waves were detected. The ECG also showed atrial fibrillation (AF), and the maximum voltage of the f wave in V_1 was 0.2 mV. The serum creatine kinase-MB fraction level was 3.4 IU/L, and the serum troponin-I level was 0.96 ng/mL. According to his family physician, the patient had an 18-month history of AF. Because of his hemodynamic instability, an intraaortic balloon pump was inserted. After obtaining his informed consent, including to the use of the infrared coagulator to treat the AF, the patient was transferred to the operating room immediately after the coronary angiography and emergency coronary artery bypass grafting was performed. The pericardium was opened through a median sternotomy, and the cardiopulmonary bypass

was established. The left ventricle was vented with a cannula inserted through the right superior pulmonary vein. Two CABGs with saphenous vein were performed, one to the left anterior descending coronary artery and the other to the left circumflex coronary artery. A left internal thoracic artery was not used because enzyme leakage was detected and it was thought that earlier revascularization would be better. Next, tapes was passed around the SVC, IVC, and the transverse sinus to achieve good left atrial exposure. A total CPB was established by snaring the tapes around the SVC and IVC.

Epicardial ablation was performed by applying the KIRC-119 infrared coagulator. The duration of the each application was 10 seconds: two ablations of 4 seconds, 2 seconds apart. Ablation was started in the RA. The root of the RAA was encircled, and the free wall of the RA was ablated from the RAA-encircling lesion to the IVC. Vertical ablation was performed from this coagulated line to the tricuspid annulus. The opposite side of the RA was ablated from the RAA-encircling lesion to the roof of the left atrium (LA), and a box lesion encircling the PV was created. Finally, the LAA was encircled, and a linear connecting lesion between the LAA-encircling lesion and the LA box lesion was created. After all of the lesions were completed, a pair of electrodes was sutured to the RAA and another pair to the free wall of the RA. Soon after returning the patient to the intensive care unit, an ECG and atrial potentials were recorded with an HPM 4500 polygraph (Fukuda Denshi, Tokyo, Japan). Two weeks later, ECGs were recorded in the same manner. The recording conditions were (1) spontaneously beating heart, (2) overdrive pacing from the RA free wall, and (3) overdrive pacing from the RAA.

The AF spontaneously converted to sinus rhythm during the operation. No potentials were detected within the RAA-encircling lesion during spontaneous beating, but the free wall of the RA exhibited potentials synchronous with the sinus rhythm (Fig.24 A). During overdrive pacing from the RA, the cardiac rhythm was synchronous with the pacing. Overdrive pacing from the RAA did not affect the cardiac rhythm, which was a sinus rhythm (Fig 24 B).

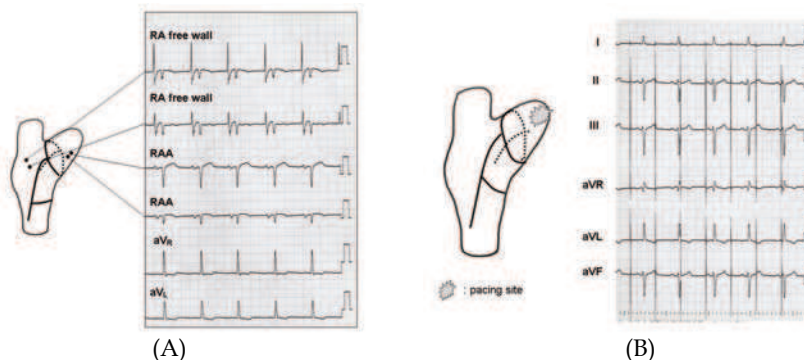(A)   (B)

Fig. 24. Atrial potentials recorded by the attached electrodes.
(A) Atrial potentials synchronous with the sinus rhythm were detected at the right atrial free wall. No atrial potentials were detected within the right atrial appendage encircling lesion. Only the small smooth curve caused by RAA movement was seen. (B) Overdrive pacing from the right atrial appendage. The pacing did not affect the cardiac rhythm.

The results of the electrophysiologic study performed 2 weeks after the operation were the same. Persistent bidirectional block was confirmed. Regular sinus rhythm was confirmed by

a postoperative 24-hour Holter monitor, and no supraventricular tachyarrhythmia was observed. An antiplatelet drug (aspirin, 81 mg/d) was started and continued. The patient recovered well, with no complications, and as of 3 years after the operation, his sinus rhythm has been maintained without the use of any antiarrhythmia drugs.

Second clinical application was performed under on-pump beating condition after ASD closure + TAP (Fig. 25). The right-side maze ablation was done epicardially. The patient restored sinus rhythm and it is maintained without antiarrhythmia drugs.

(A)

(B)

Fig. 25. Clinical application and internal appearance of the right atrial appendage in canine experiment.
(A) KIRC-119 enabled the creation of a continuous encircling transmural lesion. (B) Well-demarcated degenerated myocardium is seen. Note that all the complicated trabecular structures are discolored.

Comment

In the case reported here, the RAA was electrophysiologically isolated and the heart converted to sinus rhythm during the operation. The electrical block was confirmed immediately after the operation and again 2 weeks after the operation. We can conclude that the KIRC-119 coagulator created a continuous encircling transmural lesion in the RAA (Kubota et al., 2009).

3. Conclusions

In this chapter, the efficacy of two kinds of myocardial ablation energy source were examined and applied clinically. Using a hook-shaped cryoprobe, it was possible to create a

bidirectional conduction block in canine PVs. LAVIE technique using a conventional cryo-system was capable to a certain extent to treat non-valvular AF without prolonging aortic cross-clamp time.

Infrared energy also could make a continuous transmural lesion on the atrium in a short time. Its efficacy was confirmed experimentally, clinically and electrophysiologically. It could make a transmural lesion even on the free wall of the beating warm atrium where the cryoablation is difficult to obtain enough depth of the lesion. As next steps, accumulation of clinical cases of beating maze procedure, and development of thoracoscopic maze procedure using KIRC-119 will be considered.

4. Acknowledgement

5. References

Cox JL, Schessler RB, & Boineau JP. (1991) The surgical treatment of atrial fibrillation. I. Summary of the current concepts of the mechanisms of atrial flutter and atrial fibrillation. *J Thorac Cardiovasc Surg* 101, pp. 402–405. ISSN 00225223

Cox JL, Canavan TE, Schessler RB, Cain ME, Lindsay BD, Smith PK, Corr PB, & Boineau JP. (1991) The surgical treatment of atrial fibrillation. II. Intraoperative electrophysiologic mapping and description of the electrophysiologic basis of atrial flutter and atrial fibrillation. *J Thorac Cardiovasc Surg* 101, pp. 406–425. ISSN 00225223

Cox JL, Schessler RB, Dagostino HJ, Stone CM, Chang BC, Cain ME, Corr PB, & Boineau JP. (1991) The surgical treatment of atrial fibrillation. III. Development of a definitive surgical procedure. *J Thorac Cardiovasc Surg* 101, pp. 569–583. ISSN 00225223

Cox JL, The surgical treatment of atrial fibrillation. IV. Surgical technique. (1991) *J Thorac Cardiovasc Surg* 101, pp. 584–592. ISSN 00225223

Haïssaguerre M, Jaïs P., Shah DC, Takahashi A, Hocini M, Quiniou G, Garrigue S, Le Mouroux A,

Le Métayer P, & Clémenty J. (1998) Spontaneous initiation of atrial fibrillation by ectopic beats originating in the pulmonary veins, New Engl J Med 339, pp. 659–666., ISSN 00284793

Holman WL, Ikeshita M, Douglas JM, Smith PK, & Cox JL. (1983) Cardiac cryosurgery: effects of myocardial temperature on cryolesion size. *Surgery* 93, pp. 268–272. ISSN 00396060

Hendry PJ, Mikat EM, Anstadt MP, Plunkett MD, & and Lowe JE. Argon beam coagulation compared with cryoablation of ventricular subendocardium. *Ann Thorac Surg* 55 (1993), pp. 135–139. ISSN 00034975

Kubota H, Furuse A, Takeshita M, Kotsuka Y, & Takamoto S. (1998) Atrial ablation with an IRK- 151 infrared coagulator, Ann Thorac Surg 66, pp. 95–100. ISSN 00034975

Kubota H, Takamoto S, Takeshita M, Miyaji K, Kotsuka Y, & Furuse A. (2000) Atrial ablation using an lRK-151 infrared coagulator in canine model, *J Cardiovasc Surg* 4, pp. 835–847. ISSN 00219509

KubotaH, Takamoto S, Ohtsuka T, Nonaka K, Sato M, Fujiki K, & Sudo K. Efficacy of cryoablation in the beating heart in the treatment of atrial fibrillation, (2002) *Cardiovasc surg* 10 Suppl 1. P. 17 ISSN 09672109

Kubota H, Takamoto S, Morota T, Ohtsuka T, Motomura N, Kotsuka Y, & Sudo K. (2003) Epicardial pulmonary vein isolation by cryoablation as concomitant cardiac operation to treat nonvalvular atrial fibrillation, Ann Thorac Surg 75 pp. 590-593. ISSN 00034975

Kubota H, Takamoto s, Ohtsuka T, Endo H, Sato M, Fujiki T, & Sudo K. (2004) Epicardial pulmonary vein isolation with a hook-shaped cryoprobe to treat atrial fibrillation, *Ann Thorac Surg* 78, pp. 1056-1059. ISSN 00034975

Kubota H, Takamoto S, Furuse A, Sato M, Endo H, Fujiki T, & Sudo K. (2005) Epicardial maze procedure on the beating heart with an infrared coagulator, *Ann Thorac Surg* 80, pp. 1081–1086. ISSN 00034975

Mikat E, Hackel DB, Harrison L, Gallagher JJ, Wallace AG. (1977) Reactionof the myocardium and coronary arteries to cryosurgery. Lab. Invest 37: pp. 632-641. ISSN 00236837

Markovitz LJ, Frame LH, Josephson ME, & Hargrove WC. (1988) Cardiac cryolesions: factors affecting their size and a means of monitoring their formation. *Ann Thorac Surg* 46, pp. 531–535. ISSN 00034975

Nakajima M, Atsumi K, Furuse A, Shindo G, Kotsuka Y, & Saegusa M (1982), Studies on photocoagulation of accessory conduction pathway. *Kyobu Geka* 35, pp. 109–115. ISSN 00215252

Nath G, Kreitmair A, Kiefhaber P, & Moritz K. (1976) In: Neue infrarot-Koagulationsmethode. 9. Kongress der deutchen Gesellschaft für Endoscopie Perimed Verlag, *Erlangen*, p. 17.

Ohtake H, Watanabe G, Mukai K, Misaki T, Matsunaga Y, Matsumoto I et al. (1992) Basic study of myocardial coagulation by intraoperative laser ablation: In the presence and absence of blood. *Kyobu Geka* 45: 870-872. ISSN 00215252

Pappone C, Rosanio S, Oreto G, Tocchi M, Gugliotta F, Vicedomini G, Salvati A, Dicandia C, Mazzone P, Santinelli V, Gulletta S, & Chierchia S. (2000) Circumferential radiofrequency ablation of pulmonary vein ostia: a new anatomic approach for curing atrial fibrillation, *Circulation* 102 , pp. 2619–2628., ISSN 00097322

Svenson RH, Gallagher JJ, Selle JG, Zimmern SH, Fedor JM & Robicsek F. (1987) Neodymium: YAG laser photocoagulation: a successful new map-guided technique for the intraoperative ablation of ventricular tachycardia. Circulation 76, pp. 1319–1328. ISSN 00284793

Yamashita T, Murakawa Y, Hayami N, et al. (2000) Short-term effects of rapid pacing on mRNA level of voltage-dependent K(+) channels in rat atrium: electrical remodeling in paroxysmal atrial tachycardia. *Circulation* 25; 101: 2007-14. ISSN 00097322
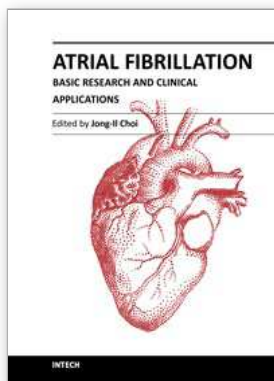
Atrial Fibrillation - Basic Research and Clinical Applications
Edited by Prof. Jong-Il Choi

Atrial Fibrillation-Basic Research and Clinical Applications is designed to provide a comprehensive review and to introduce outstanding and novel researches. This book contains 22 polished chapters and consists of five sections: 1. Basic mechanisms of initiation and maintenance of atrial fibrillation and its pathophysiology, 2. Mapping of atrial fibrillation and novel methods of signal detection. 3. Clinical prognostic predictors of atrial fibrillation and remodeling, 4. Systemic reviews of catheter-based/surgical treatment and novel targets for treatment of atrial fibrillation and 5. Atrial fibrillation in specific conditions and its complications. Each chapter updates the knowledge of atrial fibrillation, providing state-of-the art for not only scientists and clinicians who are interested in electrophysiology, but also general cardiologists.

How to reference
In order to correctly reference this scholarly work, feel free to copy and paste the following:

INTECH
open science | open minds